irregularities on the inside surface of the channel. Thus, there is a reduction in the width of the stagnation zone and, in accordance with (2), a reduction in negative pressure.

LITERATURE CITED

1. D. Rayleigh, Theory of Sound [Russian translation], Vol. 2, Moscow (1944).
2. V. G. Levich, Physicochemical Hydrodynamics, Prentice-Hall (1962).
3. A. S. Lyshevskii, Fuel Atomization in Marine Engines [in Russian], Leningrad (1971).
4. Yu. F. Dityakin, L. A. Klyachko, et al., Atomization of Liquids [in Russian], Moscow (1977).
5. I. E. Ul'yanov, Izv. Akad. Nauk SSSR, Otd. Tekh. Nauk, No. 8, 23-28 (1954).
6. V. V. Gil', Optical Methods of Studying Combustion Processes [in Russian], Minsk (1984).
7. V. V. Gil', O. G. Martynenko, S. A. Kuleshov, and K. A. Lopes-Ruiz, Second All-Union Conference on the Physics of a Low-Temperature Plasma from a Laval Nozzle, Summary of Documents, Odessa (1985), pp. 48-49.
8. A. M. Kolychev, B. S. Rinkevichus, and V. L. Chudov, Radiotekh. Élektron., 20, No. 10, 2215-2219 (1975).
9. D. T. Harry and F. G. Ridron, Instability of Combustion in a Liquid-Fuel Rocket Engine [Russian translation], Moscow (1975).
10. Ya. B. Zel'dovich, Zh. Éksp. Teor. Fiz., 12, No. 11/12, 525-538 (1942).
11. K. K. Shal'nev, Zh. Tekh. Fiz., 21, No. 2, 206-220 (1951).

NUMERICAL MODELING OF THE UNSTEADY FLOW OF A VISCOUS FLUID IN ROTATING CHANNELS

V. E. Karyakin, Yu. E. Karyakin, and A. Ya. Nesterov

UDC 532.516

A finite-difference technique is proposed for calculating flows in plane channels with arbitrary curvilinear boundaries. The technique is used to study motion in a channel with a rotating section.

Curvilinear rotating channels are an important part of modern gasdynamic equipment. As the fluid moves on the curved section of such a channel, the centrifugal forces which develop create a transverse pressure gradient. This in turn results in significant restructuring of the flow, the appearance of secondary flows, and, in some cases, the appearance of a separation region. Detailed study of these features is possible only on the basis of the Navier–Stokes equations describing the dynamics of a viscous fluid.

The investigations [1-4] numerically modeled both laminar and turbulent flow in plane channels with an angle of flow rotation of 90°. Straight sections were located before and after the rotating part. Calculations were performed in a broad range of Reynolds number and channel curvature radii. It was found that two separation regions may form; on the external wall in the rotation section; on the internal wall after the rotation section.

Several methods are available for choosing the coordinate system when calculating flows in rotating channels. One approach employs a mixed system: cartesian coordinates for the straight sections and a polar system in the rotating part [2-4]. Here, certain difficulties are encountered in attempting to combine the solutions at the boundary between the straight and rotating sections. The best coordinate system [1, 5] is one in which the boundaries of the test channel coincide with the coordinate axes. This is the system we will use in the present study.

We will examine the unsteady laminar motion of a viscous incompressible fluid in a plane channel with arbitrary curvilinear boundaries. In the Cartesian coordinate system (y_1, y_2), the flow is described as follows in dimensionless form by the Navier–Stokes equations

I. I. Polzunov Central Boiler-Turbine Institute, Leningrad.

Translated from Inzhenerno-Fizicheskii Zhurnal, Vol. 54, No. 1, pp. 25-32, January, 1988. Original article submitted August 26, 1986.

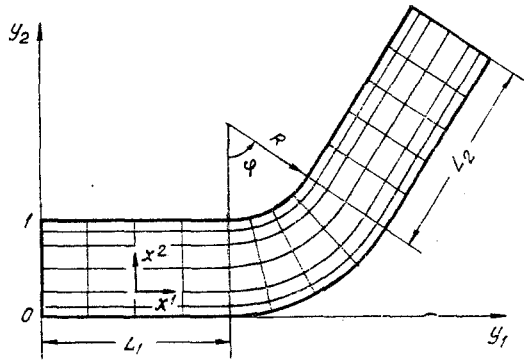

Fig. 1. Region of rotating channel.

$$\frac{\partial u_i}{\partial t}+\frac{\partial}{\partial y_k}(u_iu_k)=-\frac{\partial p}{\partial y_i}+\frac{1}{\mathrm{Re}}\frac{\partial}{\partial y_k}\left(\frac{\partial u_i}{\partial y_k}\right),\ i=1,\ 2,\ \frac{\partial u_k}{\partial y_k}=0. \tag{1}$$

Here and below, it is assumed that summation is performed from 1 to 2 over twice-repeating indices.

We introduce an arbitrary curvilinear coordinate system $x^1 = x^1(y_1, y_2)$, $x^2 = x^2(y_1, y_2)$, which transforms the test region of the flow into a square with a side equal to unity ($0 \leq x^1 \leq 1$, $0 \leq x^2 \leq 1$). In this system, it is best to write Eqs. (1) in tensor form:

$$\frac{\partial v_i}{\partial t}+\nabla_k(v_iv^k)=-\nabla_ip+\frac{g^{kl}}{\mathrm{Re}}\nabla_k(\nabla_lv_i),\quad i=1,\ 2, \tag{2}$$

$$g^{kl}\nabla_kv_l=0.$$

Here, v_i and v^i are the covariant and contravariant components of the velocity vector; ∇_i is the symbol of the covariant derivative; g^{ik} are contravariant components of the fundamental tensor [6].

Using formulas from tensor analysis, we can establish the connection between the connection between the components of the velocity vector in the coordinate systems (x^1, x^2) and (y_1, y_2):

$$v_i=u_\alpha\frac{\partial y_\alpha}{\partial x^i},\quad v^i=u_\alpha\frac{\partial x^i}{\partial y_\alpha},\quad u_i=v_\alpha\frac{\partial x^\alpha}{\partial y_i}=v^\alpha\frac{\partial y_i}{\partial x^\alpha}. \tag{3}$$

We similarly determine the tensor derivatives in Eqs. (2). The derivative ∇_kv_l is transformed as twice the covariant second-rank tensor, the derivative $\nabla_k(v_iv^k)$ is transformed as twice the covariant second-rank tensor and once the contravariant second-rank tensor, and $\nabla_k(\nabla_lv_i)$ is transformed as thrice the covariant third-rank tensor. With allowance for the above, we have:

$$\nabla_kv_l=\frac{\partial u_\alpha}{\partial y_\beta}\frac{\partial y_\beta}{\partial x^k}\frac{\partial y_\alpha}{\partial x^l}=\frac{\partial u_\alpha}{\partial x^k}\frac{\partial y_\alpha}{\partial x^l}=\frac{\partial\hat{v}_l}{\partial x^k}, \tag{4}$$

$$\nabla_k(v_iv^k)=\frac{\partial(u_\beta u_\gamma)}{\partial y_\alpha}\frac{\partial y_\alpha}{\partial x^k}\frac{\partial y_\beta}{\partial x^i}\frac{\partial x^k}{\partial y_\gamma}=\frac{\partial(u_\beta u_\gamma)}{\partial x^k}\frac{\partial y_\beta}{\partial x^i}\frac{\partial x^k}{\partial y_\gamma}=\frac{\partial(\hat{v}_i\hat{v}^k)}{\partial x^k}, \tag{5}$$

$$\begin{aligned}g^{kl}\nabla_k(\nabla_lv_i)&=\frac{\partial x^k}{\partial y_\delta}\frac{\partial x^l}{\partial y_\delta}\frac{\partial}{\partial y_\alpha}\left(\frac{\partial u_\gamma}{\partial y_\beta}\right)\frac{\partial y_\alpha}{\partial x^k}\frac{\partial y_\beta}{\partial x^l}\frac{\partial y_\gamma}{\partial x^i}=\\&=\frac{\partial x^k}{\partial y_\beta}\frac{\partial}{\partial x^k}\left(\frac{\partial u_\gamma}{\partial x^l}\frac{\partial x^l}{\partial y_\beta}\right)\frac{\partial y_\gamma}{\partial x^i}=\frac{\partial}{\partial x^k}\left(\hat{g}^{kl}\frac{\partial\hat{v}_i}{\partial x^l}\right).\end{aligned} \tag{6}$$

The symbol $(\hat{})$ is used to denote quantities calculated from the cartesian components of the velocity vector by means of matrices of the derivatives $\partial y_\alpha/\partial x^i$ and $\partial x^i/\partial y_\alpha$, fixed at the point of differentiation Q [5]:

$$\hat{v}_i=u_\alpha(\partial y_\alpha/\partial x^i)_Q=v_k\partial x^k/\partial y_\alpha(\partial y_\alpha/\partial x^i)_Q,$$

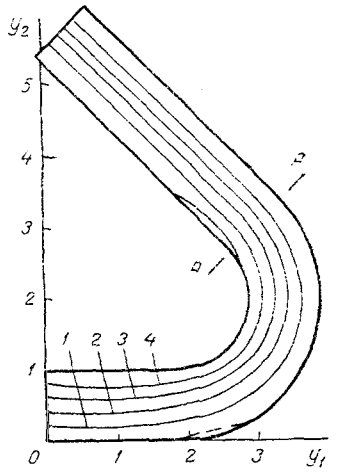

Fig. 2

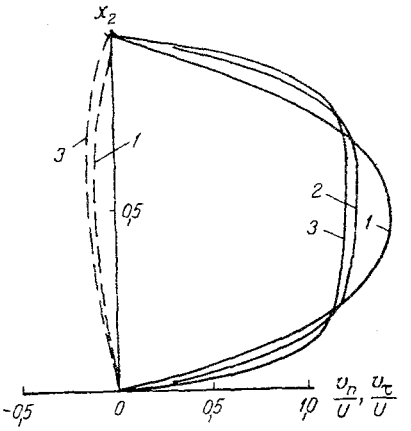

Fig. 3

Fig. 2. Streamlines in a rotating channel in the steady-state flow regime (φ = 135°, Re = 1085, R = 1, L_1 = 1.9, L_2 = 3.8): 1) ψ = 0.2; 2) 0.4; 3) 0.6; 4) 0.8. The dashed line shows the zone of reverse flow at t = 59.

Fig. 3. Profiles of the longitudinal (v_n/U, solid lines) and transverse (v_τ/U, dashed lines) physical components of the velocity vector in the section x^1 = 0.6 in the steady-state flow regime (φ = 135°, R = 1, L_1 = 1.9, L_2 = 3.8): 1) Re = 110; 2) 540; 3) 1085.

$$\hat{v}^i = v_k \hat{g}^{ik}, \quad \hat{g}^{ik} = \partial x^k / \partial y_\alpha \, (\partial x^i / \partial y_\alpha)_Q.$$

With allowance for (4-6), we can write the Navier–Stokes equations in a form not containing tensor derivatives:

$$\frac{\partial v_i}{\partial t} + \frac{\partial}{\partial x^k}(\hat{v}_i \hat{v}^k) = -\frac{\partial p}{\partial x^i} + \frac{1}{\mathrm{Re}} \frac{\partial}{\partial x^k}\left(\hat{g}^{kl} \frac{\partial \hat{v}_i}{\partial x^l}\right), \tag{7}$$

$$g^{kl} \frac{\partial \hat{v}_l}{\partial x^k} = 0. \tag{8}$$

We will use system (7-8) to calculate the flow of a fluid in a plane rotating channel with a wide inlet equal to unity (Fig. 1). We will assume that the rotating part of the channel is formed by the arcs of two concentric circles with the central angle φ. The radius of the inside wall is R. The inlet and outlet sections are formed of straight parallel walls with lengths of L_1 and L_2, respectively. The values of L_1 and L_2 were chosen so that flow in the rotating part was slightly dependent on the boundary conditions at the channel inlet and outlet.

We choose curvilinear system (x^1, x^2) so that (Fig. 1) it changes into a rectangular cartesian system on the straight sections and into a polar system on the rotating section. As the longitudinal coordinate x^1 we take the orthonormalized distance along the middle line of the channel, while the coordinate x^2 is reckoned along a normal to the outside wall. Here, all of the channel boundaries become coordinate lines. If we know the values of the coordinate x^1 for points of the inside and outside walls: $y_{1i} = y_{1i}(x^1)$, $y_{2i} = y_{2i}(x^1)$, $y_{1e} = y_{1e}(x^1)$, $y_{2e} = y_{2e}(x^1)$, then we have the following relationship between the cartesian (y_1, y_2) and curvilinear (x^1, x^2) coordinates:

$$\begin{aligned} y_1 &= [y_{1i}(x^1) - y_{1e}(x^1)]\, x^2 + y_{1e}(x^1), \\ y_2 &= [y_{2i}(x^1) - y_{2e}(x^1)]\, x^2 + y_{2e}(x^1). \end{aligned} \tag{9}$$

Using Eqs. (9), we can easily find the matrices of the derivatives $\partial y_\alpha / \partial x^i$ and $\partial x^i / \partial y_\alpha$ (i, α = 1, 2) needed for the calculations.

System (7-8) is closed by the following boundary conditions. Both components of velocity v_1 and v_2 are assigned at the channel inlet (x^1 = 0). The standard conditions of

adhesion and impermeability $v_1 = v_2 = 0$ are adopted on the solid boundaries ($x^2 = 0$ and $x^2 = 1$). At the outlet of the channel ($x^1 = 1$), we write the conditions

$$\frac{\partial}{\partial x^1} v_j \left(\frac{\partial x^j}{\partial y_1} \frac{\partial y_2}{\partial x^2} - \frac{\partial x^j}{\partial y_2} \frac{\partial y_1}{\partial x^2} \right) = 0, \qquad \frac{\partial v_2}{\partial x^1} = 0. \tag{10}$$

The first condition of (10) denotes constancy of the flow rate in a longitudinal section through an elementary cross section dx^2. For the cartesian coordinate system, conditions (10) become the usual "mild" conditions.

In solving the problem in physical variables, the pressure p is determined to within the additive constant. This constant is found from the condition: $p = 0$ at the point $x^1 = x^2 = 0$. No other boundary conditions are assigned for pressure.

To construct the difference scheme, we draw a nonuniform net $x^1 = x^1_n (n = 0, 1, \ldots, N; x^1_0 = 0, x^1_N = 1)$, $x^2 = x^2_m (m = 0, 1, \ldots, M; x^2_0 = 0, x^2_M = 1)$ in the region of integration $(0 \leq x^1 \leq 1, 0 \leq x^2 \leq 1)$. The spacing for the coordinate x^1 is chosen so as to be constant within the rotating part of the channel. In the straight sections, this spacing constantly changes in accordance with the law of geometric progression. Here, we have the denominator k_1 in the inlet part and k_2 in the outlet part. We also use a variable spacing for the coordinate x^2, with exponential condensation of the net near the channel walls. Here, the nodes of the net are found from the relation

$$2\frac{m}{M} = 1 + \frac{\ln(1 + d_1 x^2_m)}{\ln(1 + d_1)} - \frac{\ln[1 + d_2(1 - x^2_m)]}{\ln(1 + d_2)},$$

where d_1 and d_2 are parameters of the net condensation. We usually took $d_1 = d_2 = 10$ in the calculations.

The sought network functions v_1, v_2, p will be determined on nets displaced relative to each other, as is done in the marker-and-mesh method [7]. In approximating the convective terms of Eqs. (7), we will use the donor mesh scheme [7], designating the difference analog of the derivative $\partial(\hat{v}_i \hat{v}_k)/\partial x^k$ through $D_k^*(\hat{v}_i, \hat{v}^k)$. The remaining space derivatives will be approximated by second-order difference expressions. Here, we will use D_k to denote the approximation of the derivative $\partial/\partial x^k$ with respect to the adjacent nodes.

We solve system (7-8) through the use of the following implicit multistep difference scheme (the superscript n is the number of the time layer):

$$\delta v_i^{n+\frac{1}{2}}/\Delta t + D_k^*(\hat{v}_i^n, \hat{v}^{kn}) = -D_i p^n + \mathrm{Re}^{-1} D_k(\hat{g}^{kl} D_l(\hat{v}_i^n)), \tag{11}$$

$$g^{ik} D_k(\hat{v}_i^n + \delta v_i^{n+\frac{1}{2}} - \Delta t D_i(\delta p)) = 0, \tag{12}$$

$$(\delta v_i^{n+1} - \delta v_i^{n+\frac{1}{2}})/\Delta t + D_k^*(\delta v_i^{n+1}, \hat{v}^{kn}) = -D_i(\delta p) + \mathrm{Re}^{-1} D_k(\hat{g}^{kl} D_l(\delta v_i^{n+1})), \tag{13}$$

$$v_i^{n+1} = v_i^n + \delta v_i^{n+1}, \quad p^{n+1} = p^n + \delta p. \tag{14}$$

Excluding the fractional steps from Eqs. (11-14), we can show that the scheme approximates the initial system of equations (7-8) with second-order accuracy with respect to time. We will describe the main stages in the realization of this scheme.

First we use assigned values of the network functions v_1^n, v_2^n, p^n on the n-th time layer and we find preliminary corrections for the velocities $\delta v_i^{n+1/2}$ $(i = 1, 2)$ from Eqs. (11). Then using (12) – the analog of the Poisson equation for pressure – we find a correction for the pressure δp through iteration. Iteration is again used with Eq. (13) to find the final corrections for the velocities δv_i^{n+1} $(i = 1, 2)$. After this, using Eqs. (14) to effect a simple conversion, we determine the values of velocity v_i^{n+1} $(i = 1, 2)$ and pressure p^{n+1} on the new, (n + 1)-st time layer. The procedure is repeated from the very beginning for each subsequent moment of time in the unsteady problem.

The first two stages of scheme (11-14) are similar to the traditional, conditionally stable semiimplicit scheme. Completion of stage (13) makes it unnecessary to impose a strict limitation on the time step Δt.

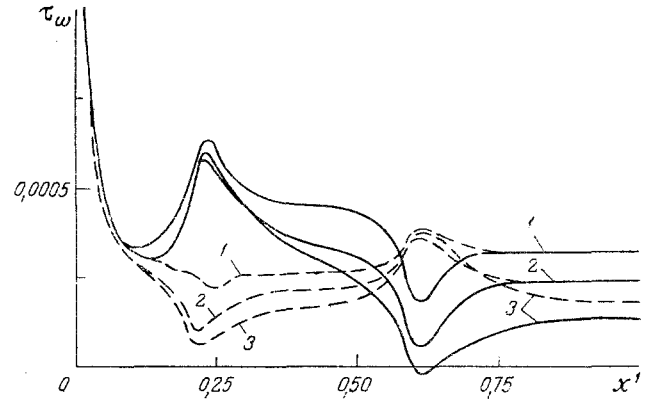

Fig. 4. Distribution of the tangential component of the dimensionless shear stress along the internal (solid lines) and external (dashed lines) walls of the channel (φ = 135°, Re = 540, R = 1, L_1 = 1.9, L_2 = 3.8): 1) t = 10; 2) 20; 3) 130.

The procedure of finding the pressure on the basis of Eq. (12) occupies the central position in the calculation of viscous flow in a channel. The method used to find this pressure should be especially efficient, since it is realized in the form of iterations on each time layer. Equation (12) is supplemented by a term with the derivative with respect to the relaxation time $\partial(\delta p)/\partial\tau$ and is solved by a splitting scheme by means of successive scalar trial runs along the directions x^1 and x^2. To speed up the iteration, we use a sequence of steps $\Delta\tau\{\Delta\tau_0, \Delta\tau_1, \ldots, \Delta\tau_s\}$ which ensures uniform convergence of the solution throughout the natural frequency spectrum of the problem. Analysis of the model equation with constant coefficients shows that in the case of an arbitrary curvilinear coordinate system, the set of steps can be obtained from the following formulas:

$$\Delta\tau_0 = \min\left[(\Delta x^1)^2/(2g^{11})\right]/\Delta t, \quad \Delta\tau_r = \Delta\tau_{r-1}/q,$$

$$q = [\pi/(4N)]^{2/s}, \quad r = 1, 2, \ldots, s.$$

A sequence of four different steps (s = 3) was usually prescribed in the calculations.

To integrate Eq. (13), we again used an iterative scheme with splitting of the space variables. The character of the splitting was determined by the flow direction, which made this approach particularly effective for studying flows with recirculation zones. As a rule, the error was reduced at least one order after each iteration in the solution of Eq. (13).

The above-described algorithm was used to calculate the viscous flow of an incompressible fluid in a rotating channel within the range of moderate Reynolds numbers 100 < Re < 1100, characterized by laminar motion of the fluid. The Reynolds number was determined from the width of the inlet section of the channel and the maximum value of the longitudinal cartesian component of velocity at the inlet. We examined different angles of channel rotation φ = 45, 90, and 135°. The radius of the inside wall of the rotating part was taken equal to R = 1. The calculations were performed on a 40 × 20 net.

We studied unsteady flows of fluid from an initial state of rest. Beginning at t = 0, at the channel inlet we assigned a uniform profile of the longitudinal cartesian component of velocity $U = U(x^2)$. The transverse velocity was assumed to be equal to zero.

Within this range of parameters, we reconstructed the development of streamline patterns and profiles of the longitudinal and transverse physical components of the velocity vector over time:

$$v_n = \frac{v^1}{\sqrt{g^{11}}} = \frac{v_1 g^{11} + v_2 g^{12}}{\sqrt{g^{11}}}, \quad v_\tau = \frac{v_2}{\sqrt{g_{22}}}, \tag{15}$$

as well as the distribution of the tangential component of the dimensionless shear stress along the channel walls:

$$\tau_w = \frac{1}{\mathrm{Re}} \frac{\sqrt{g^{22}}}{\sqrt{g_{11}}} (\nabla_2 v_1)_w, \tag{16}$$

where g_{11} and g_{22} are covariant components of the fundamental tensor.

In the case of high Reynolds numbers Re in a channel with a large angle of flow rotation φ, two zones of reverse flow develop and undergo transformation: on the external wall near the inlet in the rotating section, and on the internal wall immediately after the rotating section, and on the internal wall immediately after the rotating section. Figure 2 shows streamlines for each case of motion: Re = 1085, φ = 135°. A circulation zone is first formed on the inside wall of the channel. A similar region is then formed on the outside wall. It reaches its greatest size (shown by the dashed line) at t ≈ 60 and then gradually disappears. In this case, there is a simultaneous increase in the circulation region on the inside wall. The streamlines shown in Fig. 1 correspond to the steady-state flow regime.

Figure 3 shows profiles of longitudinal and transverse velocity in the section A—A of the channel (Fig. 2) calculated in accordance with Eqs. (15) and referred to the cartesian velocity at the inlet U. At low values of Re (Re ≈ 100), the distribution of longitudinal velocity is nearly parabolic in character. An increase in Re is accompanied by an increase in inertial forces in the core of the rotating part of the channel. This creates a transverse pressure gradient, with pressure being greater on the external wall than on the internal wall. It follows from Fig. 3 that this leads to shifting of the maximum of longitudinal velocity in the direction of the internal wall. At Re = 1085, a distinct flow core is formed along with gradient boundary regions and zones of reverse flow near the internal wall. The transverse component of velocity in the section A—A is an order lower than the longitudinal component. Some increase in this velocity can be seen with an increase in Re.

Figure 4 shows the development of the tangential shear stress along the internal and external walls of the channel over time. These results were calculated from Eq. (16) for the case Re = 540, R = 1, and φ = 135°. Near the beginning of the rotating section ($x^1 \approx 0.2$), shear stress decreases sharply on the internal wall and increases on the external wall. The opposite pattern is seen at the outlet of the rotating section ($x^1 \approx 0.6$). A certain asymmetry in the distribution of friction on the inside and outside walls is a typical feature of flows in rotating channels [1]. It also follows from the figure that at Re = 540 a short circulation zone is formed on the inside wall of the channel.

Numerical modeling of flows of liquid in channels with different angles of rotation shows that a decrease in the angle φ is accompanied by an increase in the number Re at which closed circulation regions are formed on the walls.

NOTATION

y_1, y_3, Cartesian coordinates; x^1, x^2, curvilinear coordinates; u_1, u_2, cartesian components of velocity; v_1, v_2, and v^1, v^2, covariant and contravariant components of velocity; g_{ik}, g^{ik}, covariant and contravariant components of the metrix tensor; t, time; p, pressure; φ, angle of rotation of the channel; R, radius of the inside wall; L_1, L_2, length of the inlet and outlet sections; Re, Reynolds number, N, M, number of nodes of the difference net in the longitudinal and transverse directions; d_1, d_2, k_1, k_2, net condensation parameters; Δt, time step; $\Delta\tau$, relaxation time step; τ_w, shear stress on the wall.

LITERATURE CITED

1. Orlandi and Kunsolo, Teor. Osn. Inzh. Raschetov, 101, No. 2, 202-209 (1979).
2. V. I. Grabovskii and G. B. Zhestkov, Izv. Akad. Nauk SSSR, Mekh. Zhidk. Gaza, No. 4, 20-26 (1983).
3. A. B. Vatazhin, G. B. Zhestkov, and V. A. Sepp, Izd. AN SSSR, MZhG, No. 4, 72-80 (1984).
4. R. J. Liou, M. E. Clark, J. M. Robertson, and L. G. Cheng, J. Eng. Mech., 110, No. 11, 1579-1596 (1984).
5. V. E. Karyakin and Yu. E. Karyakin, Dynamics of Nonuniform and Compressible Media (Vol. 8 of Gas Dynamics and Heat Transfer), Leningrad (1984), pp. 112-121.
6. N. E. Kochin, Vector Analysis and Introduction to Tensor Analysis [in Russian], Moscow (1965).
7. P. J. Roache, Computational Fluid Dynamics, Hermosa (1976).